

α and 3_{10} : The Split Personality of Polypeptide Helices

KIMBERLY A. BOLIN AND
GLENN L. MILLHAUSER*

Department of Chemistry and Biochemistry, University of California, Santa Cruz, California 95064

Received June 14, 1999

Introduction

Helices are ubiquitous in proteins and often the first secondary structure to emerge when a protein folds. Recent protein folding reviews focus on the importance of local interactions such as those often found in helical regions.^{1–3} Nevertheless, the mechanism by which a helix folds remains unclear. The complexity arises, in part, because there are two common helix types in polypeptides: α -helix, characterized by $i, i+4$ CO–HN hydrogen bonds, and 3_{10} -helix, characterized by $i, i+3$ hydrogen bonds. α -Helix is the most common secondary structure motif in proteins, but 3_{10} -helices are also quite common. Although 3_{10} -helix was first described by Huggins in the early 1940s,⁴ and α -helix was described by Pauling and Corey in the early 1950s,⁵ there are still numerous unanswered questions concerning their exact conformation in solution, the driving force for folding, their structural determinants, and our ability to accurately identify populations of each helix type. The interplay between the two helix types is emerging as an important issue since recent experimental and theoretical evidence suggests that 3_{10} -helix is a possible thermodynamic and/or kinetic intermediate in helix folding.

While the existence of 3_{10} -helix in structural studies is clear (see below), its identification in polypeptides by spectroscopic and computational techniques has, at times, been controversial. However, given the importance of local interactions in the early stages of protein folding, experimental investigation of these systems is of great interest and vital importance toward understanding the essentials of protein folding and design. In the following sections, we discuss the experimental and computational detection of 3_{10} -helix and emerging concepts which are changing

Kimberly Bolin received her D.Phil. in 1994 from the University of Oxford, England, after graduating with a B.A. in chemistry from Wellesley College in 1990. She was a Postdoctoral Research Fellow in the Department of Chemistry and Biochemistry at the University of California, Santa Cruz, and is currently a patent agent with the law firm of Morrison and Foerster.

Glenn L. Millhauser received a B.S. in chemistry from California State University, Los Angeles, in 1980 and a Ph.D. in chemistry from Cornell University in 1986. Supported by an NIH Fellowship, he then moved to the Pharmacology Department at Cornell to pursue postdoctoral studies. In 1988, he joined the faculty of UC Santa Cruz, where he is currently a professor in the Department of Chemistry and Biochemistry.

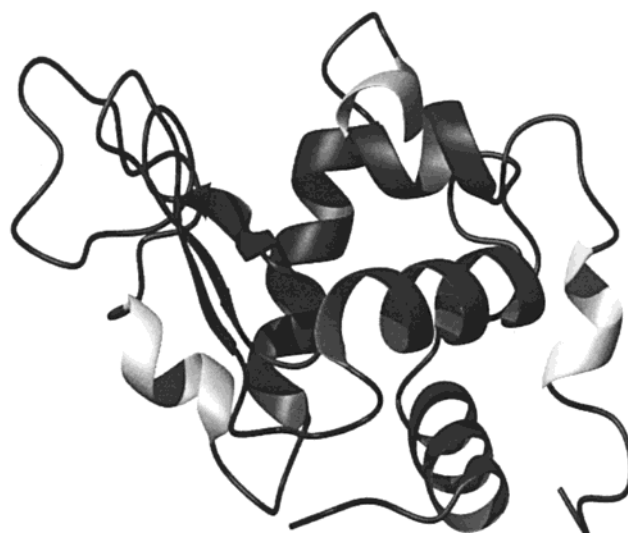


FIGURE 1. MolMol⁶¹ representation of HEWL. 3_{10} -Helices are shown in light gray, α -helices and β -sheet in dark gray. Secondary structure was determined using the program DSSP.⁶² PDB code 193I.

the most fundamental theory of protein folding: the helix–coil transition.

X-ray Crystallography

To examine the qualitative differences between α - and 3_{10} -helix, we focus first on the helix-rich protein hen egg white lysozyme (HEWL). The crystal structure of HEWL is resolved to 1.33 Å,⁶ and the protein is one of the best characterized with regard to both its structure and its folding. A mixed α/β topology (Figure 1), HEWL has seven helices and a triple-stranded β -sheet. Four of the helices adopt the α -conformation (dark gray and corresponding to residues 5–14, 25–36, 89–99, and 109–114), while the remaining three are independent 3_{10} -helices (light gray and corresponding to 80–84, 104–107, and 120–123). The collection of these helices highlights some of the contrasts between α - and 3_{10} -helix. α -Helices, at 3.6 residues/turn, tend to be longer with multiple turns, while the more tightly pitched 3_{10} -helices, at approximately 3.2 residues/turn, are shorter and usually not much longer than two turns. In addition, while the count of 3_{10} - and α -helix is comparable, as in HEWL, the total number of residues participating in 3_{10} -helix is substantially less than the number participating in α -helix. Although this balance is typical for helix-rich proteins such as HEWL, several recent structures have identified rather long 3_{10} -helices. Most notably, the structure of the leucine-rich variant shows a motif of eight alternating α - and 3_{10} -helices, with several of the 3_{10} -helices approaching nine residues in length.⁷

In the past decade or so, there have been several surveys which have taken advantage of the ever increasing number of high-resolution crystal structures to characterize protein and peptide helices. The seminal study of Barlow and Thornton⁸ was one of the first to point out

* To whom correspondence should be addressed. Voice: (831) 459-2176. Fax: (831) 459-2935. E-mail: glennm@hydrogen.ucsc.edu.

that protein helices are not as uniform as once thought. They demonstrated that α -helices show a range of conformations including kinks and curves, with only 17% identified as linear. They also demonstrated that proteins contain a significant population of 3_{10} -helices. Of the 362 helices examined by Barlow and Thornton, 71 were 3_{10} , with a mean length of 3.3 residues. As expected, protein α -helices tend to have a significantly longer mean length of 12.2 residues. If only short helical segments (≤ 6 residues) are considered, approximately 87 α -helices were identified, which is comparable to the count of 3_{10} -helices. The mean values for the backbone torsions (ϕ , ψ) were reported as -62° , -41° for α -helix and -71° , -18° for 3_{10} , though numerous studies over the years report a range of ϕ , ψ values.^{9–11}

The results of Barlow and Thornton are supported by the work of Karle and co-workers.^{12–14} Over the years, they have carefully investigated the geometry of peptides containing α -aminoisobutyric acid (Aib), a helix supporting $C_{\alpha,\alpha}$ disubstituted amino acid. In shorter peptides with one or more Aib residues, 3_{10} is favored. Karle and Balaram¹³ examined the structural trends as a function of polypeptide length and Aib content, and their work suggests that helical peptides of six residues, but lacking Aib, are equally likely to adopt a 3_{10} - or α -helical conformation.¹⁵ Furthermore, elongation of a delicately balanced 3_{10} -helix by just one amino acid can drive a facile transition to α -helix.¹⁶

Karpen et al.¹⁷ compared the amino acid distributions in the two helix types and found that certain residues, particularly Asp, appear to favor the formation of 3_{10} -helices by serving as N-caps which satisfy a further N-terminal amide hydrogen bond.¹⁸ They also noted a different distribution of hydrophobic residues between the two helix types, with hydrophobic residues at the N' (N-terminal of the N-cap) and the C-cap positions substantially stabilizing short 3_{10} -helices through packing interactions. This study suggests that the local structure determinants of α - and 3_{10} -helices are somewhat different.

Some of the first evidence for 3_{10} -helix as a folding intermediate in the formation of an α -helix was suggested by Sundaralingam and Sekharudu.¹⁹ In their study of hydrated α -helices in protein crystal structures, they observed a progressive $i+4 \rightarrow i+3 \rightarrow$ no hydrogen bond transition. Since these results were reported, numerous theoretical and experimental systems have been probed in an attempt to fully explore the nature of the helical ensemble in peptides. Several of these studies are addressed below.

Molecular Dynamics Calculations of Helical Peptides and Helix–Coil Theory

Current investigations of isolated helical secondary structure were initiated with the experimental discovery by Brown and Klee²⁰ that the C-peptide of ribonuclease A adopts helical secondary structure in aqueous solution. These studies received a further boost with the design by Marqusee and Baldwin of a short 16-residue peptide which adopts substantial helix, as measured by CD²¹ and

NMR.²² These initial investigations were the precursors to a multitude of experimental and theoretical peptide studies.

Advances in computing power and techniques now enable MD calculations to more closely approximate the time scales necessary for helix folding. Computational studies of helix folding focus on short homopolymer systems^{23–25} and also on sequences analogous to experimental systems.^{26–30} Here we highlight a few of the noteworthy examples.

Tirado-Rives and Jorgensen²⁸ were among the first to observe the formation of $i+3$ hydrogen bonding intermediates in folding simulations of the S-peptide of ribonuclease A. Since then, a number of studies have confirmed this result.^{24–26,31} For example, Sung observed multiple $i+3 \rightarrow i+4$ transitions during long MD trajectories.²⁷ These studies show that, in general, 3_{10} -turns are common during folding and often persist at the termini of α -helical domains.

The work of Brooks and co-workers^{32–37} has provided fundamental new insights into helix folding. By mapping free energy surfaces in model tripeptides, they observed stable $i+3$ and $i+4$ hydrogen bonds, thereby indicating that 3_{10} -like turns are a common part of helix initiation. Using the energies from these calculations to parametrize a new form of Zimm–Bragg theory, which allows for 3_{10} -helix, they demonstrated that 3_{10} -helix is a significantly populated folding intermediate.³⁵ A fundamental component of this model is the recognition that nucleation (i.e., formation of the first hydrogen bond) is more favorable for 3_{10} - compared to α -helix, since a turn of 3_{10} -helix requires the constraint of fewer backbone torsion angles. Interestingly, the incorporation of $i+3$ hydrogen bonds does not significantly change the shape or cooperative nature of the helix–coil transition, and this may explain why 3_{10} -helix can be missed in some experimental studies. Similar results were reported by Rohl and Doig,³⁸ who extended Lifson–Roig helix–coil theory to include even $i+5$ hydrogen bonding. While they find that the π -helical ($i, i+5$) state is not favored under any conditions, 3_{10} -helix is favored for shorter peptides, where the more favorable 3_{10} nucleation again tips the balance.

Another assumption built into most helix–coil models is that hydrogen bond propagation is equivalent at both the N- and C-termini of a helical domain. The Brooks group tested this assumption on Ala-rich peptides and showed that 3_{10} -helix propagation is more facile at the C-terminus.³⁶

Samuelson and Martyna^{29,30} have demonstrated some of the variability of MD studies depending on solvent and peptide charge. The ensemble of α - and 3_{10} -helix conformers can be affected not only by the inclusion of water in the simulation, which favors populations of 3_{10} -helical hydrogen bonds, but also by the presence or absence of positively charged Lys side chains.²⁹ When a single Lys is included in a 16- or 8-residue Ala peptide, the peptide is weakly helical in water, but in a vacuum the peptides form compact states in order to “solvate” the positive charge. In water, the Lys residues are solvated by the H₂O

molecules. These results suggest caution in widely interpreting MD results based on simulations without adequate solvent waters and based solely on homopolymer systems which are not accessible to experimental techniques.

While the previous studies simulate peptides mainly in aqueous environments, a recent study by Chipot and Pohorille³¹ explored helix folding at a water/hexane interface. Their simulation of the folding and translocation of poly-L-leucine across the water/hexane interface yields several interesting observations. While the neat solvents appeared to stabilize discrete conformations, at the water/hexane interface the peptide sampled multiple helical conformations. Throughout a 50-ns simulation, many 3_{10} -to- α and α -to- 3_{10} transitions were observed. Taken together, these theoretical studies suggest that helices exist in mixed 3_{10} and α conformations. Recent experiments lend strong support to these conclusions.

CD, NMR, and ESR of Helical Peptides

The study of helical peptides offers two unique contributions to the field of protein folding. First, because helix formation during protein folding is often rapid and within the deadtime of time-resolved techniques, partially folded peptides corresponding to native helical sequences provide insight into local folding initiation sites.^{39–44} Second, partially folded helical peptides serve as templates for exploring helix stabilizing interactions.^{45–47} For example, the 3K peptide developed by Marqusee and Baldwin forms a stable monomeric helix in aqueous solution.²¹



This peptide and similar Ala-rich sequences have been the subject of numerous spectroscopic studies. While this peptide was originally studied by CD, ESR provided the first residue-specific structural information. Using pairs of nitroxide spin-labeled Cys residues at selected positions in a series of 3K peptides, a mix of α - and 3_{10} -helix was detected.⁴⁸ These results prompted further investigation of the helix structure by NMR. (Please note that the original report on the ESR work showed a spectrum influenced by a peptide contaminant. A correction was subsequently published,⁴⁸ and correct spectra were reported in ref 15. The conclusions of the original report remain intact.)

NMR, a powerful tool for elucidating the conformations of helical peptides, offers several probes of local structure: $^3J_{\text{NH}\alpha}$ coupling constants provide the ϕ backbone torsion angle of specific residues; NOEs quantify distances between protons within $<5 \text{ \AA}$ of each other;⁴⁹ and hydrogen exchange data for backbone amide protons identifies the presence of hydrogen bonds and/or exclusion from solvent.⁵⁰ Following the identification of mixed α -/ 3_{10} -helical structure in the 3K peptide by ESR, NMR studies were undertaken on the 3K peptide and the related MW sequence, shown below.^{22,51}



The $^3J_{\text{NH}\alpha}$ coupling constants for the 3K and MW peptides are shown in Figure 2 and are consistent with

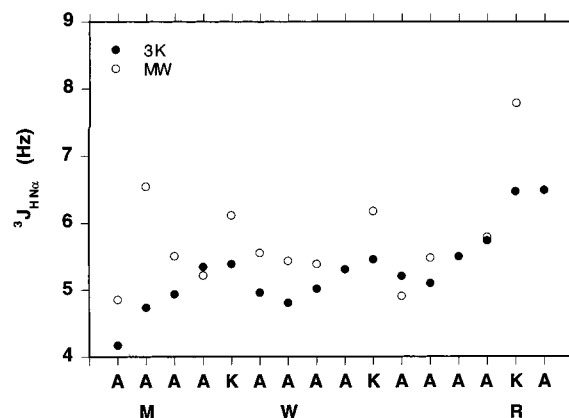


FIGURE 2. $^3J_{\text{NH}\alpha}$ coupling constants measured for the 3K (●) and MW (○) peptides at 2 °C, pH 5, in 50 mM phosphate buffer. Sequential couplings less than 6 Hz indicate well-structured helix.

significant helical structure.²² In general, four or more residues having $^3J_{\text{NH}\alpha} < 6 \text{ Hz}$ are considered indicative of helix in that region,¹¹ and for the 3K peptide only the last two residues have $^3J_{\text{NH}\alpha} > 6 \text{ Hz}$. The profile of $^3J_{\text{NH}\alpha}$ for the MW peptide is very similar to that of the 3K peptide, though the $^3J_{\text{NH}\alpha}$ are slightly greater, indicating a slightly less helical peptide, consistent with CD.⁵¹ These data suggest that the N-termini of the peptides are more stable than the C-termini, a conclusion supported by other experimental and theoretical studies.^{28,32,52–54}

The presence of persistent structure at the N-terminus and evidence for the 3_{10} -helix conformation is also indicated by 1D hydrogen–deuterium exchange data for the 3K peptide.⁵¹ Specifically, in α -helix and random coil conformations, amides 2 and 3 should not be involved in hydrogen bonds and therefore will exchange rapidly with solvent. However, if 3_{10} -helical conformers are present, there will be selective protection of amide 3. Indeed, such selective protection was observed for the 3K peptide. Similar results for a pre-nucleated model helix were reported by Zhou et al.⁵⁵

The MW peptide, with specifically placed Met and Trp residues, was designed to increase NMR signal dispersion.⁵¹ Indeed, 2D NMR spectra obtained at 750 MHz yielded diagnostic αN and $\alpha\beta$ NOEs for several regions along the helix. NOE intensities are inversely proportional to the sixth power of the distance between the proton pairs, and it is well recognized that various types of secondary structure give rise to unique NOE patterns.⁴⁹ In α - and 3_{10} -helices, the distance between the $\text{C}_\alpha\text{H}_{(i)}$ and $\text{NH}_{(i+3)}$ protons is equivalent. However, the distance between the $\text{C}_\alpha\text{H}_{(i)}$ and $\text{C}_\beta\text{H}_{(i+3)}$ protons is not, with the distance being substantially greater in the 3_{10} -helix. Therefore, the ratio of the $\alpha\beta_{(i, i+3)}/\alpha\text{N}_{(i, i+3)}$ NOEs can be related to the relative populations of α - and 3_{10} -helix. Applying this analysis to resolved pairs of $\alpha\beta_{(i, i+3)}/\alpha\text{N}_{(i, i+3)}$ NOEs from the MW peptide, a profile of the lower bound population of 3_{10} -helix can be calculated,⁵¹ as shown in Figure 3. From these data, it is apparent that, despite the uniformity of the coupling constants, there is significant variation in the population of 3_{10} -helix. The greatest proportion of 3_{10} is located at the C-terminus (66%),

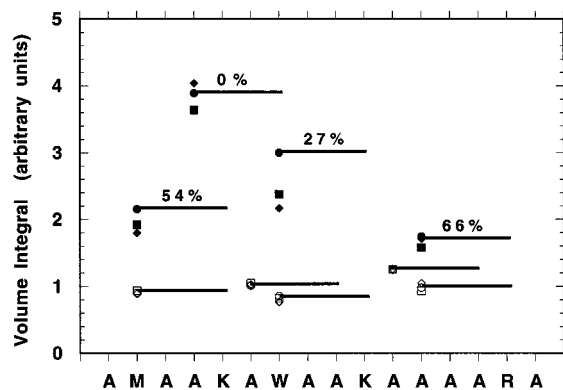


FIGURE 3. (a) Summary of $\alpha N(i, i+3)$ (open) and $\alpha\beta(i, i+3)$ (filled) NOEs in the MW peptide with mixing times of 100 (\circ , \bullet), 200 (\square , \blacksquare), and 400 ms (\diamond , \blacklozenge). Continuous lines connect the i to $i+3$ positions and are situated on the 100-ms data. For each mixing time, $\alpha N(i, i+3)$ and $\alpha\beta(i, i+3)$ were normalized so that the average $\alpha N(i, i+3) = 1$. Percentages indicate lower bound estimates of 3_{10} -helix.

though a roughly similar amount is found at the N-terminus (54%). However, even in the center of the peptide, there is a significant population (27%) of 3_{10} -helix.

Beyond the assessment of α and 3_{10} conformers, examination of Figure 3 reveals an additional and perhaps surprising result. The relative $\alpha N(i, i+3)$ intensities remain constant across the sequence, indicating that the peptide is sampling *only* helical conformations. This is supported by nearly uniform sequential NN NOEs and $^3J_{\text{NH}\alpha}$ coupling constants.⁵¹ Excursions into extended random coil conformations should significantly reduce the $\alpha N(i, i+3)$ NOE intensities at the helix termini, and this is clearly not observed. These NMR results contradict the CD results, which suggest a substantial amount of unfolded conformers for both the 3K and MW peptides. In other words, the peptide appears to exist only as a superposition of α - and 3_{10} -helix, with little contribution from random coil.

Similar results for a 3K type peptide were reported by Long and Tycko.⁵⁶ They performed a novel solid-state NMR investigation of the MB($i+4$)EK peptide with site-specific ^{13}C labeling at Ala9 and Ala14.



Figure 4 shows the quantitative analysis of the 2D magic angle spinning (MAS) NMR data in 1:1 frozen glycerol/ H_2O at -140°C (Figure 4a) and with the addition of 5.1 M urea (Figure 4b) for Ala9. The contours represent the probability that the NMR data arise from α -helix, 3_{10} -helix, and, at the origin, random coil (i.e., $f(c) = 1 - f(\alpha) - f(3_{10})$). In Figure 4a, it is apparent that Ala9 samples α -helical conformational space almost exclusively. However, upon addition of the denaturant urea, the peptide conformation shifts to largely 3_{10} -helix, with little contribution from random coil. The same results are obtained for Ala14. These results support the solution NMR findings for the MW peptide and, taken together, suggest that helical peptides which appear to be unfolded by CD criteria may actually be well structured but as a superposition of 3_{10} - and α -helix.

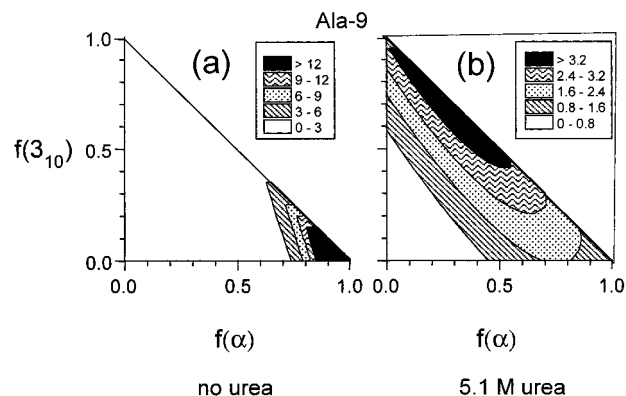


FIGURE 4. Quantitative analyses of 2D MAS NMR exchange data showing the unfolding path of the α -helical MB($i+4$)EK peptide. Contours represent the probability of α -helix and 3_{10} -helix denoted by $f(\alpha)$ and $f(3_{10})$, respectively. The random coil content is given by $f(c) = 1 - f(\alpha) - f(3_{10})$. (a) Probability for Ala9 in frozen glycerol/ H_2O at -140°C . (b) Same as (a) but with 5.1 M urea. Panel b demonstrates that a partially destabilized helical peptides exists as a superposition of α and 3_{10} , with little contribution from random coil. (Adapted from Long and Tycko⁵⁶ with permission from the authors.)

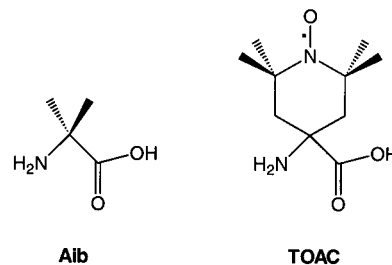


FIGURE 5. Structure of the $\text{C}_{\alpha, \alpha}$ -disubstituted amino acid Aib and its spin label analogue, TOAC.

Further ESR studies make use of TOAC, a nitroxide spin label analogue of the $\text{C}_{\alpha, \alpha}$ -disubstituted amino acid Aib (Figure 5). TOAC is rigidly attached to the peptide backbone and is therefore motionally restricted and able to report directly on the backbone environment.⁵⁷ However, like Aib,¹³ TOAC favors helical ϕ , ψ space and thus will influence the distribution of peptide conformers in the ensemble. ESR spectra of peptides in solution with selective placement of double TOAC labels show biradical interactions which reveal a hierarchy of distances consistent with 3_{10} -helix in hexamer peptides and α -helix in 16-residue peptides.^{58,59} These results are completely consistent with earlier crystallographic studies.¹³

Recent studies have focused on a quantitative evaluation of the inter-nitroxide dipolar interaction in water-soluble, double-TOAC-labeled peptides.⁶⁰ Combined CD and ESR spectra of 3K and 4K sequences suggest that both are highly structured and adopt the α -helical conformation; there is no evidence for 3_{10} -helix, and this is a consequence of the helix-stabilizing TOAC residues. The ESR line shapes are fitted with a simulation algorithm which extracts distance and relative orientation information. The expected distances for a typical α -helix are $d(i, i+3) \approx d(i, i+4)$. However, these peptides showed $d(i, i+3) > d(i, i+4)$ and inter-nitroxide distances of 8.6 and 6.6 Å for 3KT(4,7) and 3KT(4,8), respectively. Assuming

uniform backbone torsion angles throughout the peptides, these distances are consistent with a model having torsion angles of $\phi = -70^\circ$ and $\psi = -45^\circ$. In turn, these torsion angles suggest that the 3KT sequence adopts a helical conformation with 3.8–3.9 residues/turn, which is substantially more open than the canonical α -helix of 3.6 residues/turn. Computer modeling suggests that this more open geometry leaves the hydrogen bonding network intact but with an acute C'–O \cdots N angle of 140° , which results in a splaying of the backbone amide carbonyls away from the helix axis and into solution. This type of local structure appears to be unique for soluble helical peptides, and this open geometry may be favored because it simultaneously accommodates the hydrogen bonding network while allowing for solvation of the amide carbonyls. Thus, even the expected α -helical geometry of 3.6 residues/turn, as commonly found in protein α -helices, may not be the preferred conformation for solvated Ala-rich helical peptides.

Conclusions

It appears that polypeptide helices do, indeed, have a split personality. They can be either α or 3_{10} , depending on length, sequence, local packing, or even just random chance—and partially folded peptides can dynamically switch between the two conformers. Barlow and Thornton's⁸ survey was the first to suggest the wide range of helix geometries, and it has since become apparent that there are significant equilibrium populations of 3_{10} -helix in both proteins and peptides. A consistent and emerging perspective, supported by MD, ESR, and NMR, suggests that 3_{10} -helix is also an intermediate on the folding pathway to well-structured α -helix,^{15,51,56} and thus short stretches of 3_{10} -helix are an expected structural component.^{27,28,35,36,38} Given that the two helix types were initially identified over 40 years ago, and that helix is a major component of folded proteins, it is rather surprising that the interplay between α and 3_{10} is just now becoming clear. In addition, experiments are suggesting new interpretations of CD data and previously unsuspected open structures for solvated helical peptides. And while split personalities are not always desirable, they certainly add new and unexpected twists to polypeptide structures.

This work was supported by grants from the NIH (GM46870), the UC Biotechnology Program (97-18), and the Petroleum Research Fund (32164-AC4), administered by the ACS. K.A.B. and G.L.M. thank the donors of the PRF for their support. In addition, the authors thank Dr. R. Tycko for generously providing the data shown in Figure 4.

References

- (1) Baldwin, R. L.; Rose, G. D. Is protein folding hierarchic? I. Local structure and peptide folding. *Trends Biochem. Sci.* **1999**, *24*, 26–33.
- (2) Baldwin, R. L.; Rose, G. D. Is protein folding hierarchic? II. Folding intermediates and transition states. *Trends Biochem. Sci.* **1999**, *24*, 77–83.
- (3) Aurora, R.; Creamer, T. P.; Srinivasan, R.; Rose, G. D. Local interactions in protein folding: lessons from the alpha-helix. *J. Biol. Chem.* **1997**, *272*, 1413–1416.
- (4) Huggins, M. L. The Structure of Fibrous Proteins. *Chem. Rev.* **1943**, *32*, 195–218.
- (5) Pauling, L.; Corey, R. B.; Branson, H. R. The Structure of Proteins: Two Hydrogen-Bonded Helical Conformations of the Polypeptide Chain. *Proc. Natl. Acad. Sci. U.S.A.* **1951**, *37*, 205–211.
- (6) Vaney, M. C.; Maignan, S.; Rieskautt, M.; Ducruix, A. High-Resolution Structure (1.33-Angstrom) Of a Hew Lysozyme Tetragonal Crystal Grown In the Apcf Apparatus—Data and Structural Comparison With a Crystal Grown Under Microgravity From Spacehab-01 Mission. *Acta Crystallogr. Sect. D: Biol. Crystallogr.* **1996**, *52*, 505–517.
- (7) Peters, J. W.; Stowell, M. H.; Rees, D. C. A leucine-rich repeat variant with a novel repetitive protein structural motif [letter]. *Nat. Struct. Biol.* **1996**, *3*, 991–994.
- (8) Barlow, D. J.; Thornton, J. M. Helix Geometry in Proteins. *J. Mol. Biol.* **1988**, *201*, 601–619.
- (9) Ramachandran, G. N.; Sasisekharan, V. Conformation of Polypeptides and Proteins. *Adv. Protein Chem.* **1968**, *23*, 283–437.
- (10) Toniolo, C.; Benedetti, E. The polypeptide 3_{10} -helix. *Trends Biochem. Sci.* **1991**, *16*, 350–353.
- (11) Smith, L. J.; Bolin, K. A.; Schwalbe, H.; MacArthur, M. W.; Thornton, J. M.; Dobson, C. M. Analysis of Main Chain Torsion Angles in Proteins: Prediction of NMR Coupling Constants for Native and Random Coil Conformations. *J. Mol. Biol.* **1996**, *255*, 494–506.
- (12) Karle, I. L.; Flippenanderson, J. L.; Uma, K.; Balam, P. Apolar Peptide Models For Conformational Heterogeneity, Hydration, and Packing Of Polypeptide Helices—Crystal Structure Of Heptapeptides and Octapeptides Containing Alpha-Aminoisobutyric Acid. *Proteins: Struct., Funct. Genet.* **1990**, *7*, 62–73.
- (13) Karle, I. L.; Balam, P. Structural Characteristics Of Alpha-Helical Peptide Molecules Containing Aib Residues. *Biochemistry* **1990**, *29*, 6747–6756.
- (14) Karle, I. L. Flexibility in Peptide Molecules and Restraints Imposed by Hydrogen Bonds, the AIB Residue, and Core Inserts. *Biopolymers* **1996**, *40*, 157–180.
- (15) Millhauser, G. L. Views of Helical Peptides: A Proposal for the Position of 3_{10} Helix along the Thermodynamic Folding Pathway. *Biochemistry* **1995**, *34*, 3873–3877.
- (16) Karle, I. L.; Flippen-Anderson, J. L.; Gurunath, R.; Balam, P. Facile transition between $3(10)$ - and alpha-helix: structures of 8-, 9-, and 10-residue peptides containing the -(Leu-Aib-Ala)₂-Phe-Aib-fragment. *Protein Sci.* **1994**, *3*, 1547–1555.
- (17) Karpen, M. E.; de Haseth, P. L.; Neet, K. E. Differences in the amino acid distributions of $3(10)$ -helices and alpha-helices. *Protein Sci.* **1992**, *1*, 1333–1342.
- (18) Aurora, R.; Rose, G. D. Helix capping. *Protein Sci.* **1998**, *7*, 21–38.
- (19) Sundaralingam, M.; Sekharudu, Y. C. Water-inserted alpha-helical segments implicate reverse turns as folding intermediates. *Science* **1989**, *244*, 1333–1337.
- (20) Brown, J. E.; Klee, W. A. Helix-Coil Transition of the Isolated Amino Terminus of Ribonuclease. *Biochemistry* **1971**, *10*, 470–476.

- (21) Marqusee, S.; Robbins, V. H.; Baldwin, R. L. Unusually stable helix formation in short alanine-based peptides. *Proc. Natl. Acad. Sci. U.S.A.* **1989**, *86*, 5286–5290.
- (22) Millhauser, G. L.; Stenland, C. J.; Bolin, K. A.; Ven, F. J. M. v. d. Local Helix Content in an Alanine-Rich Peptide as Determined by the Complete Set of $^3J_{\text{HN}\alpha}$ Coupling Constants. *J. Biomol. NMR* **1996**, *7*, 331–334.
- (23) Tirado-Rives, J.; Maxwell, D. S.; Jorgensen, W. L. Molecular Dynamics and Monte Carlo Simulations Favor the α -Helical Form for Alanine-Based Peptides in Water. *J. Am. Chem. Soc.* **1993**, *115*, 11590–11593.
- (24) Bertsch, R. A.; Vaidehi, N.; Chan, S. I.; Goddard, W. A. Kinetic steps for alpha-helix formation. *Proteins: Struct., Funct. Genet.* **1998**, *33*, 343–357.
- (25) Takano, M.; Yamato, T.; Higo, J.; Suyama, A.; Nagayama, K. Molecular dynamics of a 15-residue poly(L-alanine) in water: Helix formation and energetics. *J. Am. Chem. Soc.* **1999**, *121*, 605–612.
- (26) Soman, K. V.; Karimi, A.; Case, D. A. Unfolding Of an Alpha-Helix In Water. *Biopolymers* **1991**, *31*, 1351–1361.
- (27) Sung, S. S. Folding Simulations Of Alanine-Based Peptides With Lysine Residues. *Biophys. J.* **1995**, *68*, 826–834.
- (28) Tirado-Rives, J.; Jorgensen, W. L. Molecular dynamics simulations of the unfolding of an alpha-helical analogue of ribonuclease A S-peptide in water. *Biochemistry* **1991**, *30*, 3864–3871.
- (29) Samuelson, S.; Martyna, G. J. Computer simulation studies of finite temperature conformational equilibrium in alanine-based peptides. *J. Phys. Chem. B* **1999**, *103*, 1752–1766.
- (30) Samuelson, S. O.; Martyna, G. J. Two-dimensional umbrella sampling techniques for the computer simulation study of helical peptides at thermal equilibrium: The 3K(I) peptide in vacuo and solution. *J. Chem. Phys.* **1998**, *109*, 11061–11073.
- (31) Chipot, C.; Pohorille, A. Folding and translocation of the undecamer of poly-L-leucine across the water-hexane interface. A molecular dynamics study. *J. Am. Chem. Soc.* **1998**, *120*, 11912–11924.
- (32) Tobias, D. J.; Brooks, C. L. d. Thermodynamics and mechanism of alpha helix initiation in alanine and valine peptides. *Biochemistry* **1991**, *30*, 6059–6070.
- (33) Tobias, D. J.; Mertz, J. E.; Brooks, C. L. d. Nanosecond time scale folding dynamics of a pentapeptide in water. *Biochemistry* **1991**, *30*, 6054–6058.
- (34) Brooks, C. L. I.; Case, D. A. Simulations of Peptide Conformational Dynamics and Thermodynamics. *Chem. Rev.* **1993**, *93*, 2487–2502.
- (35) Sheinerman, F. B.; Brooks, C. L. 310 Helices in Peptides and Proteins as Studied by Modified Zimm-Bragg Theory. *J. Am. Chem. Soc.* **1995**, *117*, 10098–10103.
- (36) Young, W. S.; (III) C. L. B. A Microscopic View of Helix Propagation: N and C-terminal Helix Growth in Alanine Helices. *J. Mol. Biol.* **1996**, *259*, 560–572.
- (37) Brooks, C. L. Helix-Coil Kinetics—Folding Time Scales For Helical Peptides From a Sequential Kinetic Model. *J. Phys. Chem.* **1996**, *100*, 2546–2549.
- (38) Rohl, C. A.; Doig, A. J. Models For the 3(10)-Helix/Coil, Pi-Helix/Coil, and Alpha-Helix/3(10)-Helix/Coil Transitions In Isolated Peptides. *Protein Sci.* **1996**, *5*, 1687–1696.
- (39) Dyson, H. J.; Merutka, G.; Waltho, J. P.; Lerner, R. A.; Wright, P. E. Folding of Peptide Fragments Comprising the Complete Sequence Of proteins—Models For Initiation of Protein Folding 1. Myohe-merythrin. *J. Mol. Biol.* **1992**, *226*, 795–817.
- (40) Dyson, H. J.; Sayre, J. R.; Merutka, G.; Shin, H. C.; Lerner, R. A.; Wright, P. E. Folding Of Peptide Fragments Comprising the Complete Sequence of proteins—Models For Initiation Of Protein Folding 2. Plastocyanin. *J. Mol. Biol.* **1992**, *226*, 819–835.
- (41) Dyson, H. J.; Wright, P. E. Peptide Conformation and Protein Folding. *Curr. Opin. Struct. Biol.* **1993**, *3*, 60–65.
- (42) Yang, J. J.; Buck, M.; Pitkeathly, M.; Kotik, M.; Haynie, D. T.; Dobson, C. M.; Radford, S. E. Conformational properties of four peptides spanning the sequence of hen lysozyme. *J. Mol. Biol.* **1995**, *252*, 483–491.
- (43) Kuhlman, B.; Boice, J. A.; We, W.-J.; Fairman, R.; Raleigh, D. P. Calcium Binding Peptides from α -Lactalbumin: Implications for Protein Folding and Stability. *Biochemistry* **1997**, *36*, 4607–4615.
- (44) Ruiz-Sanz, J.; de Prat Gay, G.; Otzen, D. E.; Fersht, A. R. Protein Fragments as Models for Events in Protein Folding Pathways: Protein Engineering Analysis of the Association of Two Complementary Fragments of the Barley Chymotrypsin Inhibitor 2 (CI-2). *Biochemistry* **1995**, *34*, 1695–1701.
- (45) Bierzynski, A.; Kim, P. S.; Baldwin, R. L. A Salt Bridge Stabilizes the Helix Formed by the Isolated C-Peptide of RNase A. *Proc. Natl. Acad. Sci. U.S.A.* **1982**, *79*, 2470–2474.
- (46) Stellwagen, E.; Park, S. H.; Shalongo, W.; Jain, A. The contribution of residue ion pairs to the helical stability of a model peptide. *Biopolymers* **1992**, *32*, 1193–200.
- (47) Trulson, J. A.; Millhauser, G. L. The effect of mutations on peptide models of the DNA binding helix of p53: Evidence for a correlation between structure and tumorigenesis. *Biopolymers* **1999**, *49*, 215–224.
- (48) Miick, S. M.; Martinez, G. V.; Fiori, W. R.; Todd, A. P.; Millhauser, G. L. Short alanine-based peptides may form 3_{10} -helices and not α -helices in aqueous solution. *Nature (London)* **1992**, *359*, 653–655; *Nature (London)* **1992**, *377*, 257 (correction).
- (49) Wüthrich, K. *NMR of Proteins and Nucleic Acids*; John Wiley & Sons: New York, 1986.
- (50) Bai, Y. W.; Milne, J. S.; Mayne, L.; Englander, S. W. Primary Structure Effects On Peptide Group Hydrogen Exchange. *Proteins: Struct., Funct. Genet.* **1993**, *17*, 75–86.
- (51) Millhauser, G. L.; Stenland, C. J.; Hanson, P.; Bolin, K. A.; Ven, F. J. M. v. d. Estimating the Relative Populations of 3_{10} -Helix and α -Helix in Ala-rich Peptides: A Hydrogen Exchange and High Field NMR Study. *J. Mol. Biol.* **1997**, *267*, 963–974.
- (52) Miick, S. M.; Casteel, K. M.; Millhauser, G. L. Experimental Molecular Dynamics of an Alanine-Based Helical Peptide Determined by Spin Label Electron Spin Resonance. *Biochemistry* **1993**, *32*, 8014–8021.
- (53) Doig, A. J.; Chakrabarty, A.; Klingler, T. M.; Baldwin, R. L. Determination of free energies of N-capping in alpha-helices by modification of the Lifson-Roig helix-coil theory to include N- and C-capping. *Biochemistry* **1994**, *33*, 3396–3403.
- (54) Karle, I. L.; Flippen-Anderson, J. L.; Uma, K.; Balaram, P. Unfolding of an alpha-helix in peptide crystals by solvation: conformational fragility in a heptapeptide. *Biopolymers* **1993**, *33*, 827–837.

- (55) Zhou, H. X. X.; Hull, L. A.; Kallenbach, N. R.; Mayne, L.; Bai, Y. W.; Englander, S. W. Quantitative Evaluation Of Stabilizing Interactions In a Prenucleated Alpha-Helix By Hydrogen Exchange. *J. Am. Chem. Soc.* **1994**, *116*, 6482–6483.
- (56) Long, H. W.; Tycko, R. Biopolymer conformational distributions from solid-state NMR: alpha-helix and 3(10)-helix contents of a helical peptide. *J. Am. Chem. Soc.* **1998**, *120*, 7039–7048.
- (57) Toniolo, C.; Valente, E.; Formaggio, F.; Crisma, M.; Pilloni, G.; Corvaja, C.; Toffoletti, A.; Martinez, G. V.; Hanson, M. P.; Millhauser, G. L.; et al. Synthesis and conformational studies of peptides containing TOAC, a spin-labelled C alpha, alpha-disubstituted glycine. *J. Pept. Sci.* **1995**, *1*, 45–57.
- (58) Hanson, P.; Martinez, G.; Millhauser, G.; Formaggio, F.; Crisma, M.; Toniolo, C.; Vita, C. Distinguishing helix conformations in Alanine-rich peptides using the unnatural amino acid TOAC and electron spin resonance. *J. Am. Chem. Soc.* **1996**, *118*, 271–272.
- (59) Hanson, P.; Millhauser, G.; Formaggio, F.; Crisma, M.; Toniolo, C. ESR Characterization Of Hexameric, Helical Peptides Using Double Toac Spin Labeling. *J. Am. Chem. Soc.* **1996**, *118*, 7618–7625.
- (60) Hanson, P.; Anderson, D. J.; Martinez, G.; Millhauser, G.; Formaggio, F.; Crisma, M.; Toniolo, C.; Vita, C. Electron spin resonance and structural analysis of water soluble, alanine-rich peptides incorporating TOAC. *Mol. Phys.* **1998**, *95*, 957–966.
- (61) Koradi, R.; Billeter, M.; Wüthrich, K. MOLMOL: a program for display and analysis of macromolecular structures. *J. Mol. Graphics* **1996**, *14*, 51–55.
- (62) Kabsch, W.; Sander, C. Dictionary of protein secondary structure: pattern recognition of hydrogen-bonded and geometrical features. *Biopolymers* **1983**, *22*, 2577–2637.

AR980065V